Sixth International Symposium on Turbulence and Shear Flow Phenomena
Seoul, Korea, 22-24 June 2009

NUMERICAL SIMULATION OF SELF-PROPELLED AQUATIC SWIMMING IN UNIFORM AND VORTICAL FLOWS

Iman Borazjani
St. Anthony Falls Laboratory,
University of Minnesota
2 Third Ave SE, Minneapolis, Minnesota 55414, USA
boraz002@umn.edu

Fotis Sotiropoulos
St. Anthony Falls Laboratory,
University of Minnesota
2 Third Ave SE, Minneapolis, Minnesota 55414, USA
fotis@umn.edu

ABSTRACT

Fish swimming has fascinated scientists for a long time but important questions regarding the effect of scale (Reynolds number), body shape and kinematics, and approach flow on swimming performance still remain unanswered. In this paper we review our previous computational work with tethered and self-propelled virtual swimmers in a free stream and present new results of tethered swimmers in the wake of a cylinder in order to provide answers to some of these questions. The work with tethered swimmers showed that carangiform swimmers (e.g. mackerel) are more efficient in the inertial regime while anguilliform swimmers (e.g. lamprey) are more efficient in the transitional regime. To isolate the effects of body shape and kinematics, we created two hybrid virtual swimmers—a mackerel swimming like lamprey and a lamprey swimming like a mackerel—and made them race each other in the same hydrodynamic environment by performing self-propelled simulations. We found that the mackerel body always reached higher velocities in all flow regimes but is more efficient only in the inertial regime. The lamprey body was found to be more efficient in the transitional regime. The lamprey kinematics reached higher velocities and was more efficient in the transitional regime while the mackerel kinematics in the inertial regime. The simulations of a tethered mackerel in the wake of a circular cylinder show that the cylinder wake gives rise to larger thrust-type force relative to that of the same mackerel swimming in uniform ambient flow.

INTRODUCTION

Aquatic fishlike swimming has been the subject of intense study not only for its scientific/biological value but also to help engineer biomimetically inspired vehicles and propulsive systems. Depending on their size and swimming speed, fishes swim across a range of Reynolds numbers (Re) spanning the viscous, transitional and inertial regimes. Smaller fish or fish in the larvae stage swim at low Re of order 10^0 to 10^3 while larger adult swimmers such as Dolphins can swim at Re as high as 10^6. Some fishes, such as eel or zebrafish larvae, swimming at relatively lower Re~10^4, use the anguilliform mode for swimming while others, such as mackerel or tuna, swimming at relatively higher Re~10^5, use the carangiform mode—see Sfakiotakis et al. (1999) for the definitions of different modes of swimming. Studying the hydrodynamics of these mode of swimming and comparing their performance at different Re with experiments alone is a challenging task due to difficulties obtaining the 3D flow and pressure fields around the fish and controlling live animals (Tytell, 2007). Numerical simulations, on the other hand, do not suffer from these experimental difficulties but are very challenging due to, among others, the complex geometry, thin flexible moving bodies, non-linear fluid-structure interaction (FSI) phenomena, and the high computational costs for resolving biologically relevant scales. Consequently, relatively few numerical simulations have been attempted to date—see Borazjani et al. (2008) for a review.

In this paper we apply the FSI solver developed by our group (Borazjani et al., 2008) (see also (Ge and Sotiropoulos, 2007; Gilmanov and Sotiropoulos, 2005)) to study fishlike swimming. We present an overview of our recent work with tethered carangiform (mackerel) (Borazjani and Sotiropoulos, 2008) and anguilliform (lamprey) (Borazjani and Sotiropoulos, 2009a) swimmers in uniform flow to study the hydrodynamics of the two modes of swimming over a range of Reynolds and Strouhal numbers. To further test the effect of kinematics vs. body shape both swimming kinematics are prescribed to both mackerel and lamprey bodies and used to carry out self-propelled simulations in a stagnant ambient flow (see Fig 1). We study the effect of kinematics by comparing the swimmers with the same body. Similarly, we study the effect of body shape by comparing the swimmers with the same kinematics. Finally we also explore the performance of a tethered swimmer in a vortical ambient flow by carrying out simulations of a mackerel swimming in the wake of a circular cylinder.

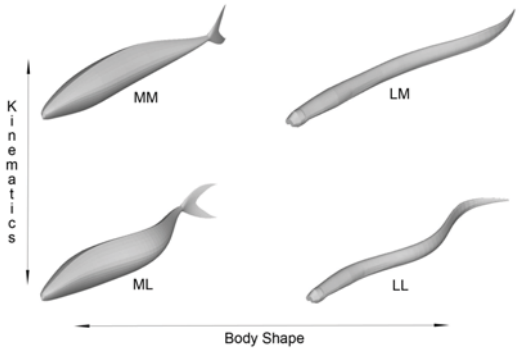

Fig. 1 Four different virtual swimmers. Each row have the same kinematics while each column have the same body. A) mackerel swimming like a mackerel (MM); B) lamprey swimming like a mackerel (LM); C) mackerel swimming like a lamprey (ML); D) lamprey swimming like lamprey (LL).

NUMERICAL METHODS

Flow Solver

The equations governing the fluid motion are solved via a the curvilinear/immersed boundary (CURVIB) method, which is capable of carrying out direct numerical simulation of flows with complex moving boundaries (Ge and Sotiropoulos, 2007). The fluid equations are integrated in time using an efficient, second-order accurate fractional step methodology coupled with a Jacobian-free, Newton–Krylov solver for the momentum equations and a GMRES solver enhanced with multigrid as pre-conditioner for the Poisson equation (Ge and Sotiropoulos, 2007).

For the self-propelled simulations the fluid equations were solved in the frame of reference attached to the fish center of mass i.e. non-inertial frame of reference (Borazjani, 2008; Borazjani and Sotiropoulos, 2009b).

The fish moving body is handled with a sharp-interface immersed boundary method (Gilmanov and Sotiropoulos, 2005). The method blanks out the nodes inside the immersed bodies and reconstructs the boundary conditions on the fluid nodes in the immediate vicinity of immersed boundary (IB nodes) using a quadratic interpolation (Gilmanov and Sotiropoulos, 2005). The quadratic reconstruction has been shown to be 2nd order accurate (Gilmanov and Sotiropoulos, 2005). The background grid nodes are first classified into fluid, solid, and IB nodes using an efficient ray-tracing algorithm (Borazjani et al., 2008).

Self-propelled Simulations

For self-propelled simulations the non-inertial reference frame is attached to the virtual swimmers center of mass. The motion of the center of mass is obtained by solving the Newton's 2nd law of motion (momentum) equations for the fish in non-dimensional form:

$$M_{red}\frac{d\mathbf{U}}{dt} = C_F \tag{1}$$

where $\mathbf{U}$ is the fish swimming speed vector non-dimensionalized by U^1, $M_{red}=m/\rho L^3$ is the reduced mass (where m is the mass of the virtual swimmer and ρ is the fluid density), and $C_F=F/\rho(U^1)^2L^2$ is the force coefficient (where $\mathbf{F}$ is the force vector exerted on the virtual swimmer's body by the fluid). In this work the virtual swimmer is restricted to swim only along the streamwise direction. The position of the non-inertial frame is obtained by solving the following equation:

$$\frac{d\mathbf{x}_c}{dt} = \mathbf{U} \tag{2}$$

where $\mathbf{x}_c$ is the position vector of center of mass non-dimensionalized by L, i.e. the position of the origin of the non-inertial frame relative to the inertial frame.

FSI Coupling Method

The FSI problem is solved through a partitioned approach, within which the problem is partitioned into two separated domains: one fluid and one structural domain. Both the loose and strong coupling strategies are implemented to resolve the interaction between the fluid flow and the leaflet motions (Borazjani et al., 2008).

Due to relatively small reduced mass and a strong added mass effect the FSI couplings will be unstable. To achieve stability with strong coupling the solutions had to be under-relaxed (Borazjani et al., 2008). The value of under-relaxation parameter plays an important role in the convergence and efficiency of the strong coupling and was calculated dynamically via the Aitken acceleration method (Borazjani et al., 2008).

Fish Body Kinematics and Non-dimensional Parameters

The bodies of the virtual swimmers are exactly the same as those used in our previous tethered simulations (Fig. 1). The carangiform body was modeled after the actual anatomy of a mackerel (Borazjani and Sotiropoulos, 2008) while the anguilliform body was created from a lamprey computed tomography (CT) scan by Professor Frank Fish provided to us by Professor Lex Smits from Princeton University (Borazjani and Sotiropoulos, 2009a).

The kinematics for body/caudal-fin (BCF) locomotion is generally in the form of a backward traveling wave as follows (all lengths are non-dimensionalized with the fish length L):

$$h(z,t) = a(z)\sin(kz - \omega t) \tag{3}$$

In the above equation: z is the axial (swimming) direction measured along the fish axis from the tip of the fish head; $h(z,t)$ is the lateral excursion of the body at time t; $a(z)$ is the amplitude envelope of lateral motion as a function of z; k is the wave number of the body undulations that corresponds to a wavelength λ; and ω is the angular frequency. Both modes of BCF propulsion studied herein, i.e. anguilliform and carangiform, are described by the above traveling wave Eqn. (3) by choosing an amplitude envelope $a(z)$ and a wave length λ (or wave number k), referred to hereafter as *shape parameters*, that match that mode of swimming.

The amplitude envelope $a(z)$ for the anguilliform kinematics was approximated by an exponential function (Borazjani and Sotiropoulos, 2009a; Tytell and Lauder, 2004):

$$a(z) = a_{\max} e^{z-1} \quad (4)$$

For carangiform kinematics the amplitude envelop was approximated by a quadratic curve of the form (Borazjani and Sotiropoulos, 2009a):

$$a(z)=a_0+a_1 z+a_2 z^2 \quad (5)$$

For a typical anguilliform fish the coefficient a_{max} is set equal to a_{max}=0.1 (Hultmark et al., 2007). The following values are used for the coefficients $a_0=0.02$, $a_1=-0.08$ and $a_2=0.16$ to match the experimental curve of Videler and Hess (1984) for typical carangiform kinematics. Both kinematics have the maximum displacement at the tail $a_{\max}$=0.1, i.e. $h_{\max}=0.1L$. The wave number k in all simulations is based on the non-dimensional wavelength λ/L = 0.642 for anguilliform (Borazjani and Sotiropoulos, 2009a; Hultmark et al., 2007) and λ/L = 0.95 for carangiform (Borazjani and Sotiropoulos, 2008; Videler and Hess, 1984) swimmers.

The four important non-dimensional similarity parameters in fishlike swimming are: 1) the Reynolds number $Re=UD/\upsilon$; 2) the Strouhal number based on the maximum lateral excursion of the tail $A=2h_{\max}$, and the tail beat frequency f: $St=2fh_{\max}/U$; 3) the non-dimensional wavelength λ/L; and 4) the non-dimensional amplitude envelope $a(z/L)/L$. Sometimes the so-called slip velocity or slip ratio, defined as $slip=U/V=U/(\omega/k)$, is used instead of non-dimensional wavelength. Using either parameter is correct. However, the slip velocity changes if the tail beat frequency is changed, while the wavelength and the tail beat frequency are independent.

Computational Details

For tethered simulations the virtual swimmers are towed with constant swimming speed U and tail beat frequency is changed. By fixing the speed U, we fix the Reynolds number and by changing the frequency for a specific speed we vary the Strouhal number. The simulations are performed at Re=300, 4000 and ∞ (inviscid). For each Re, the St is increased until the force on the virtual tether is of thrust-type. For self-propelled simulations the virtual swimmers start to undulate in an initially stagnant fluid and the swimming speed is determined based on the forces on the fish body. Therefore, Re and St change until the quasi-steady state is reached. The swimmers are released in three different environments with different fluid viscosity: 1) a very viscous fluid that results in a quasi-stationary state with a mean Re~300; 2) a moderately viscous fluid with Re~4000; 3) an inviscid fluid (Re=∞). For the sake of convenience and from the numerical standpoint it is desirable that the resulting mean swimming speed U be close to unity. Therefore, the tail beat frequency in each swimming environment is selected close to the critical St^* found in the tethered carangiform simulations (Borazjani and Sotiropoulos, 2008) for which the net average force F was zero. The reduced mass M_{red} is set equal to 0.01 for all of virtual swimmers.

The computational domain and time step for the self-propelled mackerel and lamprey body simulations in the free stream are exactly the same as the tethered mackerel simulations (Borazjani and Sotiropoulos, 2008) and tethered lamprey simulations (Borazjani and Sotiropoulos, 2009a), respectively, with about 5million grid nodes. The computational domain is a cuboid with dimensions $2L\times L\times 7L$, which is discretized with 5.5 million grid nodes. The domain width $2L$ and height L are more than fifteen times the lamprey width $0.067L$ and height $0.066L$, and ten times the mackerel width $0.2L$ and height $0.1L$, respectively. The fish is placed $1.5L$ from the inlet plane in the axial direction and centered in the transverse and the vertical directions.

The domain for simulations of a tethered mackerel behind the cylinder is $8D\times 2D\times 18D$ with $225\times 101\times 353$ grid nodes. A fine mesh with spacing $h=0.016D$ in a cuboid with dimensions $2D\times D\times 2D$ contains the mackerel at all times. The mackerel is placed $2D$ behind the cylinder. The simulations are performed at Re=150 and 2000 based on cylinder diameter and free stream velocity.

RESULTS

Tethered Virtual Swimmers

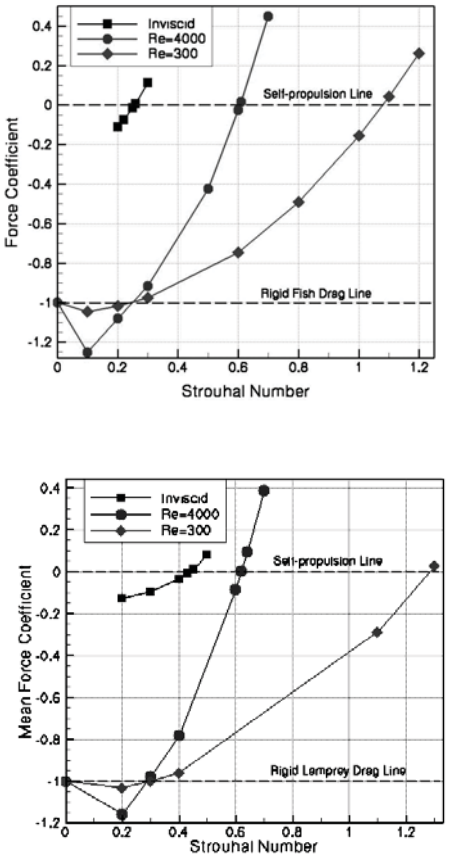

Fig. 2 Effect of Reynolds and Strouhal numbers on the mean force coefficient produced by the tethered mackerel (top) and lamprey (bottom). The force coefficient is time-averaged and normalized by the rigid body drag coefficient. The lower dash line shows the rigid body drag coefficient and the upper dash line shows the zero mean force coefficient i.e. self-propulsion limit. Taken from (Borazjani and Sotiropoulos, 2008, 2009a).

Simulations were performed at Re=300, 4000 and inviscid and for each Re the St was increased from 0.1 until the average force on the tether was of thrust-type (Borazjani and Sotiropoulos, 2008, 2009a). The average force coefficient vs. St for different Re is shown in Fig. 2. It can be observed that for each Re, at low St the fish initially produces more drag than the rigid (non-undulating) fish but as St is increased the force coefficient decreases and finally crosses the self-propulsion line, where the mean force is zero. The St at self-propulsion limit is named the critical St^*. The reason for the initial larger drag-type force than the rigid fish is that at low St the body wave speed V is lower than the towing speed U, which causes the flow to separate from the fish body (Borazjani and Sotiropoulos, 2008, 2009a). However, by increasing the St the body wave speed is increased and when $V>U$ the separation is eliminated.

It can be also observed that St^* is a decreasing function of Re. The Froude efficiency is calculated at the Strouhal number at which the swimmers can self-propel themselves, i.e. at St^*. For the mackerel the efficiency is 18.86%, 22.95%, and 47.55% and for the lamprey 17.62%, 31.62%, and 18.89% at Re=300, 4000, and inviscid, respectively. The power required for self-propulsion was found to be higher than the power required for towing the rigid fish at the same Re and decreased as Re increased. The power required for self-propulsion of the lamprey was found to be smaller than that of the mackerel at the same Re. The force coefficient fluctuations of the mackerel were found to be higher than that of the lamprey. These differences can be due to difference in either body shape or kinematics of the lamprey and mackerel, which will be discussed in next section.

Self-propelled Virtual Swimmers

As discussed in the computational details section, for a given hydrodynamic environment (fixed viscosity) all four virtual swimmers are released with the same tail beat frequency and the self-propelled, FSI simulations are continued until the swimmers reach quasi-steady state. The calculated time series of swimming speeds for the three hydrodynamic environments and for all four swimmers are shown in Figs. 3. It can be observed that the swimmers with mackerel body (MM and ML. where the first letter denotes the body shape, Mackerel or Lamprey, and the second letter denotes the kinematics) always reach higher velocities. Comparing the swimmers with the same body we observe that the swimmer with anguilliform kinematics (ML and LL) reach higher velocities in the viscous and transitional while the ones with carangiform kinematics (MM and LM) reach higher velocities in the inertial regime. It is interesting to note that even in the inertial regime initially the anguilliform kinematics is ahead but later the carangiform kinematics takes over and reaches higher velocity in the steady state.

To quantify swimming efficiency, we calculate the power spent by the swimmers in the final quasi-steady state. We find that the swimmers with anguilliform kinematics have higher efficiency than the carangiform ones in the viscous and transitional regimes i.e. $\eta_{MM}=22.1< \eta_{ML}=26.3$ and $\eta_{LM}=26.4<\eta_{LL}=32.1$ at Re~4000. On the other hand the swimmers with carangiform kinematics are more efficient in the inertial regime i.e. $\eta_{MM}=45.0> \eta_{ML}=37.9$ and $\eta_{LM}=19.4> \eta_{LL}=18.9$ in inviscid simulations. To explore the effect of body shape we note that the swimmers with mackerel body are more efficient in the inertial regime than the swimmers with lamprey body i.e. $\eta_{MM}=45.0> \eta_{LM}=19.4$ and $\eta_{ML}=37.9>\eta_{LL}=18.9$ in inviscid simulations. Instead, in the transitional regime the swimmers with lamprey body are more efficient i.e. $\eta_{MM}=22.1<\eta_{LM}=26.4$ and

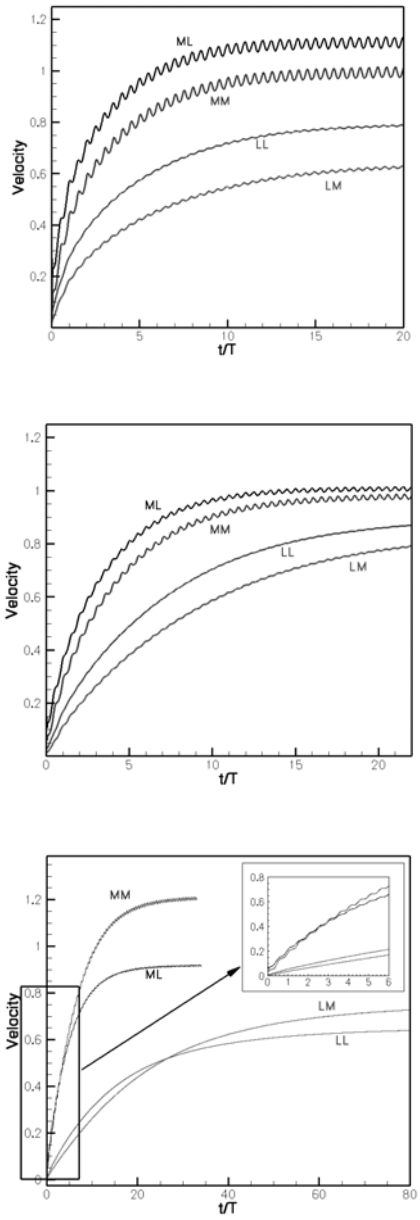

Fig. 3 Swimming speed time history of the virtual swimmers in viscous Re~300 (top), transitional Re~4000 (middle), and inertial (inviscid bottom) regimes. See Fig. 1 for definition of swimmer MM, ML, LM, and LL. Taken from (Borazjani and Sotiropoulos, 2009b).

η_{ML}=26.3<η_{LL}=32.1 at Re~4000. For more details the reader is referred to (Borazjani, 2008; Borazjani and Sotiropoulos, 2009b)

Tethered Virtual Swimmer behind a Cylinder

All previous simulations were performed in a uniform approach flow. To start exploring the effect of approach flow conditions on swimming performance, we place a tethered mackerel at distance *2D* behind a cylinder in different positions (center, middle, and edge) in the wake as shown in Fig. 4. The simulations are performed at Re=150 and 2000 based on the cylinder diameter and free stream velocity.

Fig. 5 shows the force coefficient time history for different fish positions behind the cylinder along with that on the fish swimming in the free stream at the same Re and St. It is readily observed that the force coefficient on the tethered fish is strongly affected by the approach flow. As seen in Fig. 5, the force record clearly exhibits a frequency lower than the tail beat frequency that corresponds to the vortex-shedding frequency. Note that the force coefficient of the fish swimming in the free stream is periodic with zero mean while those in the wake of the cylinder show great deviations with a positive (thrust-type) mean. This suggests that the fish needs less power to stay stationary in the wake of the cylinder than in a free stream at the same Re. This can be due to several reasons. First, the effective velocity in the wake is smaller than the free stream velocity, which will decrease the effective Re and increase the effective St for the fish. Second, the vortices shed from the cylinder create a low pressure region in the front part of the fish, which increase the force coefficient (see Fig. 6). Third, the interaction of the vortices shed from the cylinder with the vortices shed from the tail interacts in ways that possibly enhance thrust production. To what extent the above reasons affect the force coefficient is not known and further research is required to identify the wake/fish interaction mechanisms that lead to the apparent enhancement of thrust production.

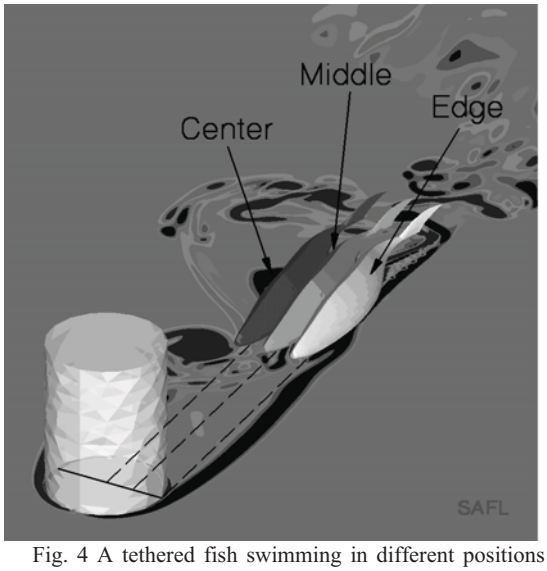

Fig. 4 A tethered fish swimming in different positions behind a cylinder. The flow is visualized by the out-of-plane vorticity in the midplane of the fish in the edge position behind the cylinder (Re=2000, St=0.6).

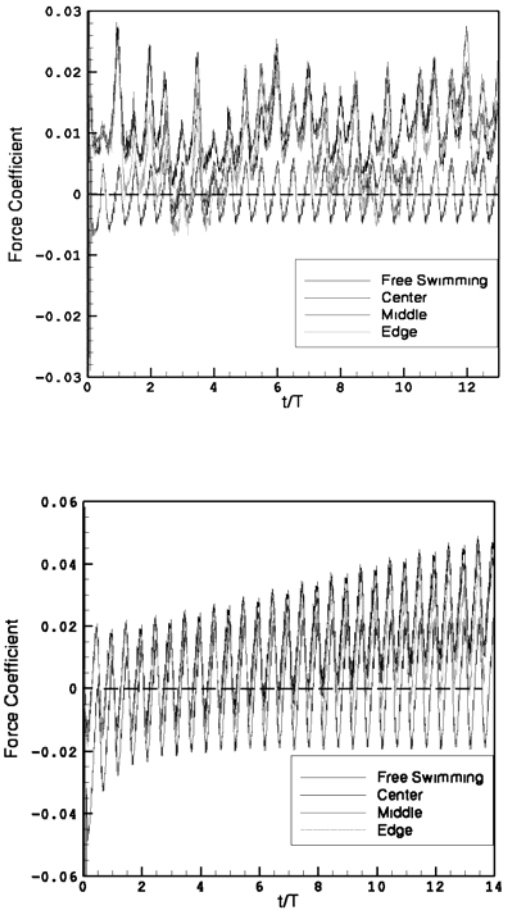

Fig. 5 The time history of the force coefficient for different fish positions behind the cylinder along with a swimming in a free stream is provided for Re=2000, St=0.6 (top) and Re=150, St=1.1 (bottom).

CONCLUSIONS AND FUTURE WORK

We employed virtual swimmers to study aspects of aquatic swimming that are not possible to study by experiments with live fish. We have answered some important question regarding the effect of Re and St on the performance of the swimming and the effect of kinematics and body shape in this regard. For tethered swimmers we showed that for a given body shape and kinematics there is a unique Stouhal number (St^*) for each Re at which self-propelled swimming is possible (Borazjani and Sotiropoulos, 2008, 2009a). This St^* is a decreasing function of Re and explains why fishes such Pacific salmon swim at higher St, out of the normal rage 0.2 to 0.35, at low swimming speeds (Borazjani and Sotiropoulos,2008, 2009a). Furthermore, we found that the mackerel efficiency increases as Re is increased while the lamprey efficiency is peaked in the transitional regime (higher than the mackerel) and decreases as Re is increased. The power required for

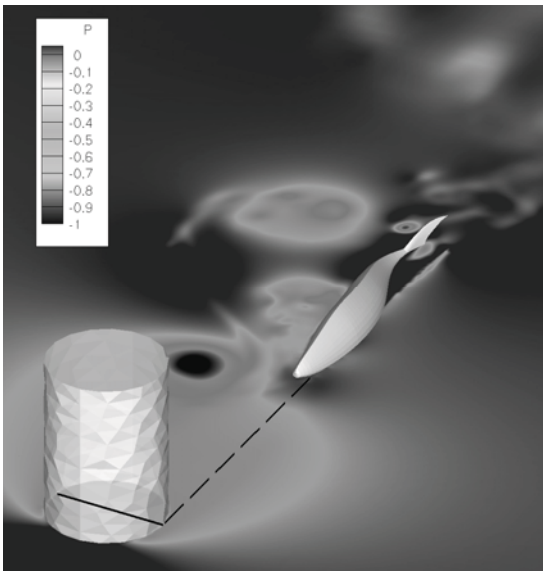

Fig. 6 The pressure field in the midplane of the fish in the edge position behind the cylinder (Re=2000, St=0.6).

self-propulsion for both tethered mackerel and lamprey were higher than towing the rigid fish at the same Re and decreased as Re is increased. The power required for self-propulsion of the lamprey was lower than the mackerel (Borazjani and Sotiropoulos, 2008, 2009a). The force coefficient was found to be much smoother for the lamprey relative to the mackerel, which explained the lower velocity fluctuations for anguilliform swimmers relative to carangiform swimmers observed in experiments (Borazjani and Sotiropoulos, 2008, 2009a). These differences between the mackerel and lamprey can be due either body shape or kinematics. To study the effect of body shape and kinematics we preformed self-propelled simulation of four virtual swimmers (a mackerel, a lamprey, a mackerel swimming like a lamprey, and a lamprey swimming like mackerel) racing each other (Borazjani, 2008; Borazjani and Sotiropoulos, 2009b). By comparing the swimmer with the same body shape but different kinematics we studied the effect of kinematics. Similarly, by comparing the swimmer with same kinematics but different body shape we studied the effect body shape. We found that the lamprey kinematics reached higher velocities and was more efficient in the transitional regime while the mackerel kinematics in the inertial regime. Moreover, we found that the mackerel body always reached higher velocities in all flow regimes but was more efficient only in the inertial regime. The lamprey body was found to be more efficient in the transitional regime.

The aforementioned simulations were performed in a free stream. To start exploring all important effects of approach flow conditions on the swimming performance, we tethered a mackerel two diameters behind a cylinder and found that the force coefficient was larger (more thrust) relative to a fish in the free stream. The vortices shed from the cylinder impinge on the anterior of the fish creating pockets of lower pressure that increase the force coefficient. In addition, the effective Re and St of a fish swimming in the wake of the cylinder is different than those in the corresponding free stream simulation. Finally, vortices shed from the cylinder interact with and are altered by the body undulations in ways that could possibly enhance thrust production. Which of the above affects is the major culprit for the observed increase of hydrodynamic thrust is not presently understood and will be the focus of our future work in this area.

ACKNOWLDEGEMENTS

This work was supported by NSF Grants 0625976 and EAR-0120914 and the Minnesota Supercomputing Institute. We are grateful to Professor Smits at Princeton University for providing the lamprey morphology data from the CT scan of Professor Fish.

REFERENCES

Borazjani, I., 2008, *Numerical Simulations of Fluid-Structure Interaction Problems in Biological Flows*, PhD Thesis, University of Minnesota, Twin Cities.

Borazjani, I., Ge, L. and Sotiropoulos, F., 2008, "Curvilinear Immersed Boundary Method for Simulating Fluid Structure Interaction with Complex 3D Rigid Bodies", *Journal of Computational physics,* Vol. 227, pp. 7587-7620

Borazjani, I. and Sotiropoulos, F., 2008, "Numerical investigation of the hydrodynamics of carangiform swimming in the transitional and inertial flow regimes", *Journal of Experimental Biology,* Vol. 211, pp. 1541-1558.

Borazjani, I. and Sotiropoulos, F., 2009a, "Numerical investigation of the hydrodynamics of anguilliform swimming in the transitional and inertial flow regimes", *Journal of Experimental Biology,* Vol. 212, pp. 576-592.

Borazjani, I. and Sotiropoulos, F., 2009b, "On the role of form and kinematics on the hydrodynamics of body/caudal fin swimming", *Journal of Experimental Biology,* Vol. submitted pp.

Ge, L. and Sotiropoulos, F., 2007, "A Numerical Method for Solving the 3D Unsteady Incompressible Navier-Stokes Equations in Curvilinear Domains with Complex Immersed Boundaries", *Journal of Computational Physics,* Vol. 225, pp. 1782–1809.

Gilmanov, A. and Sotiropoulos, F., 2005, "A hybrid Cartesian/immersed boundary method for simulating flows with 3D, geometrically complex, moving bodies", *Journal of Computational Physics,* Vol. 207, pp. 457-492.

Hultmark, M., Leftwich, M. and Smits, A., 2007, "Flowfield measurements in the wake of a robotic lamprey", *Experiments in Fluids,* Vol. 43, pp. 683.

Sfakiotakis, M., Lane, D. M. and Davies, J. B. C., 1999, "Review of fish swimming modes for aquatic locomotion", *IEEE Journal of Oceanic Engineering,* Vol. 24, pp. 237.

Tytell, E., 2007, "Do trout swim better than eels? Challenges for estimating performance based on the wake of self-propelled bodies", *Experiments in Fluids,* Vol. 43, pp. 701--712.

Tytell, E. D. and Lauder, G. V., 2004, "The hydrodynamics of eel swimming I. Wake structure", *Journal of Experimental Biology,* Vol. 207, pp. 1825.

Videler, J. J. and Hess, F., 1984, "Fast continuous swimming of two pelagic predators, saithe (Pollachius virens) and mackerel (Scomber scombrus): a kinematic analysis", *Journal of experimental biology,* Vol. 109, pp. 209.